Testing the applicability limits of a membrane distillation process with ceramic hydrophobized membranes: The critical wetting temperature

TESTING THE APPLICABILITY LIMITS OF A MEMBRANE DISTILLATION PROCESS WITH CERAMIC HYDROPHOBIZED MEMBRANES: THE CRITICAL WETTING TEMPERATURE

*Felipe Varela-Corredor and Serena Bandini**

Department of Civil, Chemical, Environmental and Materials Engineering- DICAM
Alma Mater Studiorum – University of Bologna – School of Engineering and Architecture
Via U. Terracini, 28, I-40131, Bologna, Italy

(*) corresponding author
e-mail : serena.bandini@unibo.it
tel +39 051 2090231

Key Words: critical wetting temperature, ceramic membrane contactors, liquid entry pressure, liquid entry temperature, normalized flooding curves

HIGHLIGHTS

- The new concept of the c*ritical wetting temperature* ($T_{C\ wetting}$) is introduced.
- The $T_{C\ wetting}$ is the maximum temperature to operate Membrane Distillation
- The existence of $T_{C\ wetting}$ is experimentally documented
- Hydrophobic carbon-based titania membranes show a $T_{C\ wetting}$ close to 130°C **with water**
- LET_{min} measurements are the most suitable to calculate the $T_{C\ wetting}$

ABSTRACT

The new concept of the *critical wetting temperature* ($T_{C\ wetting}$) of a hydrophobic membrane is introduced. It represents the maximum temperature at which a hydrophobic membrane can operate in no-wetting conditions with a specific liquid. The concept relies on the theoretical premises **of** the Laplace-Young equation.

The existence of the critical wetting temperature is experimentally documented for the case of carbon-based titania membranes hydrophobized with FAS, by measuring the minimum Liquid Entry Pressure values as a function of temperature, in the range from 20 °C to 136 °C. In that case, the $T_{Cwetting}$ was obtained close to 130 °C **with pure water**.

The new parameter should be included in the membrane characterization protocols, **since** t**he** evaluation **of** $\boldsymbol{T_{C\ wetting}}$ is crucial to define which are the applicability limits of a membrane contactor. In alternative to various LEP measurements as a function of temperature, the measure of the minimum Liquid Entry Temperature **at very low pressures** can represent a **more efficient** method for the $T_{Cwetting}$ evaluation.

1. INTRODUCTION

The recent renewed interest of the scientific community for Membrane Distillation **(MD)** has been favored by the development of new ceramic membranes, **which are** appropriately modified **on the** surface to give the correct hydrophobic character required for the operations [1-13]. With respect to polymeric membranes, ceramic membranes allow high thermal and chemical stability as well as a **better** morphological stability. Their use at high temperatures, also greater than 100 °C, is considered interesting for stripping operations (above all in case of low-volatile solutes) and/or for desalting applications, for example, in view of the possibility to achieve higher fluxes and to increase the salts solubility. However, **to date,** membrane wetting is the main drawback **of MD applications since it** limits the process performances and often forces the process to stop [14-24]. When MD is correctly operated, a liquid-vapor interface is typically immobilized at the pore mouth **of the hydrophobic membrane**: **since** the liquid feed **cannot enter the pore, it** vaporizes **at the interface** and vapors diffuse across the membrane. **In the case in which** the **total** pressure difference across the membrane overcomes a threshold value, the so-called *minimum Liquid Entry Pressure* (LEP_{min}), the larger pores **are** flooded of the liquid feed. **A**s the pressure increases**, an increasing number of pores can be rapidly wetted:** the separation efficiency of the membrane vanishes and the process can be restarted only after an accurate **regeneration of the membrane according to a** drying procedure. It is a matter of fact that determining the breakthrough conditions of a membrane with a specific feed is fundamental to test the applicability of the membrane **itself**, **as well as of the whole module,** for MD operations [25-27].

Typically, the selection of a membrane as element of a good membrane contactor is made by testing the material hydrophobicity with contact angle measurements at room temperature and by measuring the LEP_{min} **with pure water or with a specific solution (isopropyl alcohol-water solutions are often used) at room temperature. However, the** structure and **the** surface morphology **of the membrane (such as** pore radius distribution, pore shape, surface roughness **and** heterogeneity**) as well as t**he operating conditions can reverse the initial expectations: high temperatures, liquids with low surface tension, **traces** of surfactants and detergents, fouling and scaling can be all responsible of a rapid and unexpected membrane wetting [17,19-24,28].

Investigation of the wetting mechanism **on** polymeric membranes has been recently introduced in a systematic way by Jacob et al. [14, 15], who studied the progress of the wetting front "at pore

level". **M**ost of the papers focus on the investigation of the phenomena at room temperature**; however** the need of testing the membrane applicability at high temperatures should be considered as a real need, above all in the case of ceramic membranes which are typically proposed for operations at high temperatures. To the best of our knowledge, only Saffarini et al. [23] and Varela-Corredor&Bandini [27] performed LEP_{min} measurements on PTFE samples up to 70 °C, obtaining a sensible decrease of that quantity with respect to the values observed at room temperature. **However, Sirkar and coworkers [29] reported the use of PTFE flat sheets in Direct Contact MD for brine desalination at temperatures up to 128 °C, with no membrane wetting.** In reference [27]**, in addition,** some values of LEP_{min} were documented **alsob**for hydrophobized ceramic membranes at temperatures in the range from 90 to 100 °C.

It is well known that breakthrough conditions **can be well** described by the Laplace-Young equation, as modified by Franken et al. [**30**,25,26], in which the LEP_{min} is related to the liquid-vapor surface tension, to the maximum pore size and to the liquid-solid contact angle, by using a geometrical factor accounting of the irregularities of the **membrane** pores. In order to study how temperature affects the breakthrough conditions, attention should be focused **both** on the contact angle (which is directly related to the membrane material and pore morphology) and on the thermodynamic properties of the fluid (which affect**s** the liquid-vapor surface tension).

The dependence of surface tension on temperature is well known from Thermodynamics which documents a decreasing trend with temperature up to zero at the critical point of the substance [**31,32**].

Conversely, the role of temperature on contact angle is a problem under investigation since 1965 [3**3**]. It is an important feature in material science, since contact angle measurements are generally used to calculate the surface free energy (typically indicated as γ_{SV}) and then to estimate the solid-liquid interfacial free energy (typically indicated as γ_{SL}) basing on the Young equation [**34**]. Unfortunately, **the** measurement **of the contact angle at high temperature** is a **very** complex and delicate **operation** [**35**], although it is rather easy to be **carried out** at room temperature on flat surfaces. Experimental measurements of contact angles (advancing and/or receding) with different liquids (water, polar and un-polar organics) on **flat surfaces of** various materials (polymers, aluminum and stainless steel) are reported in [**33-39**] in a wide range of temperatures. All authors document**ed** sensible decreasing trends of contact angle**s** with temperature, typically according to a linear behavior, in the range from 20 to 160 °C. **In addition, with regards to water, authors**

observed that at temperatures higher than 120-130 °C the contact angle sharply **decreased** with temperature, showing a remarkable change of the slope with respect to the behavior **obtained below 120 C**. That effect **occurred** both on polymers, such as fluoropolymer and/or polyethylene [**35**], showing hydrophobic characteristics, and on metals [**38,39**], showing hydrophilic characteristics. In the case of fluoropolymers (poly-tetrafluoroethylene-co-hexafluoropropylene, DuPont brand) [**35**], contact angles greater than 100° (typical of hydrophobic materials) were measured up to 80 °C, whereas a contact angle of 80° was observed at 160°C, documenting a **remarkable** loss of hydrophobicity.

Although papers [33-39] dealt with contact angles on flat smooth surfaces, it is possible to argue that, in case of membranes, the combined effect of temperature on the surface tension and on the contact angle **can** lead **to a decrease of** the LEP_{min} with temperature. **Therefore, the solely** LEP_{min} **measurement** at room temperature cannot be considered a good representation of the membrane characteristics**,** as it is generally accepted by many authors [1-7,**40**]. Since **the** contact angle measurements as a function of temperature are rather difficult to be performed on hollow fibers and on capillary modules, the LEP_{min} measurement as a function of temperature seems to be the only feasible and simple way to study the role of temperature on the applicability of membrane contactors.

Aim of this work is to discuss how high temperatures affect the breakthrough conditions of a membrane contactor and to draw general indications. Firstly, the new concept of the *critical wetting temperature* is introduced, according to the premises of the Laplace-Young equation. That temperature **will be** recognized as the maximum operating temperature at which a hydrophobic membrane can operate in no-wetting conditions and its dependence on the membrane material **will be** demonstrated. Secondly, the existence of that limiting condition **will be** experimentally documented, by measuring the *minimum Liquid Entry Pressure* (LEP_{min}) and the *minimum Liquid Entry Temperature* (LET_{min}) of hydrophobized carbon-based ceramic membranes (according to the normalized-flooding-curve method introduced in [27]). Various samples of the same basic material **will be** used, manufactured in different shapes (single-channels and capillary bundles) and with different mean pore sizes; the samples **will be** tested in the temperature range from 20 to 136 °C.

2. THEORETICAL PREMISES: The critical wetting temperature

From the theoretical point of view, the LEP_{min} can be related to temperature, as well as to the membrane material and morphology, by the modified Laplace-Young equation as reported in Eq. (1).

$$\frac{LEP_{\min} \times d_{P,\max}}{4B} = \gamma_{SV}(T) - \gamma_{SL}(T) = \gamma_{LV}(T) \times \left|\cos\theta(T)\right| \quad (1)$$

decreasing function with T ***decreasing function with θ from 150° to 90°***

B is the geometrical factor accounting of the irregularities/morphology of the pores, originally introduced by Franken et al. [**30**], θ is the contact angle, γ are the free energies at the corresponding interfaces [25,**30**], $d_{P,max}$ represents the maximum pore diameter or maximum pore size.

The right hand side of Eq. (1) depends on the liquid **solution type (type of components and composition)** and on the membrane material, through the surface tension of the liquid (γ_{LV}) and the contact angle. For a given liquid **solution** and for the same membrane material, those quantities depend only on temperature. The surface tension of the liquid is typically a decreasing function with temperature [**31,32**], whereas the contact angle may depend on temperature with different trends owing to different contributions. According to what has been measured in [**33-39**], the contact angle on flat smooth surfaces greatly decreases with temperature. In addition, **in the case of macroporous membranes,** it can be affected by the pore size and by the surface morphology also [25, **41**], which **in turn** can vary with temperature owing to swelling phenomena, for instance. However, in the case in which the morphology can be considered unaffected by temperature, as it can be presumed for hydrofobized ceramic membranes, we can **approximate** the right hand side of Eq. (1) **as** a decreasing **function with temperature.** Indeed, **it can be easily recognized that the absolute value of $cos\theta$ is a decreasing function with θ ,** when the contact angle decreases with temperature **varying** from 150 to 90 degrees.

A simulation of an hypothetical trend of the right hand side of Eq.(1) with temperature, with pure water, is reported as an example in Figure 1, for various cases. The role of the membrane material is simulated according to the following assumptions:

i) The contact angles at room temperature are contained in the range from 120 to 150 degrees, as documented by many authors for ceramic membranes grafted with FAS [1,2,4-7,**40**];

ii) in the range from 150 to 90 degrees the contact angle decreases with temperature, according to a linear behavior, as documented by Petke&Ray on **various materials [35]**;

iii) any variation of **the** pore morphology with temperature is neglected (representative case of ceramic membranes).

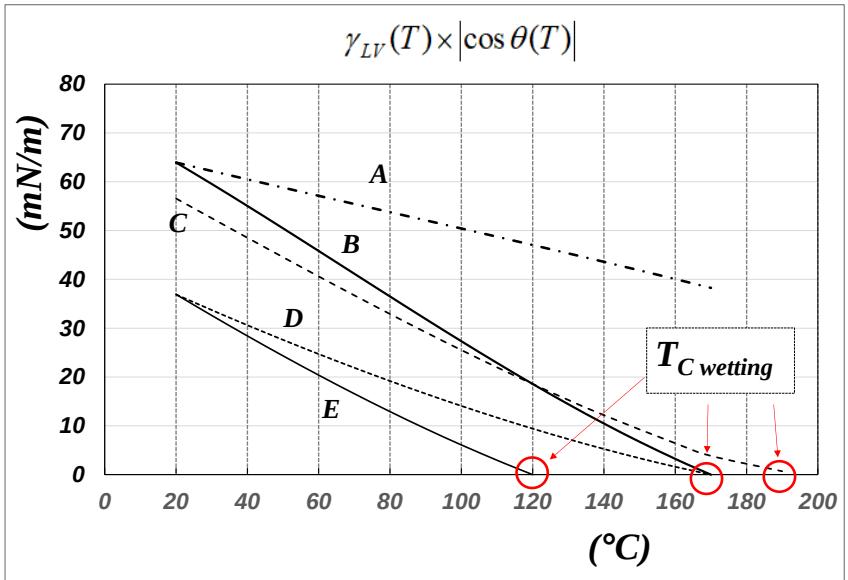

	A	B	C	D	E
θ @ 20°C (deg)	150 °	150 °	140 °	120 °	120 °
$d\theta/dT$ (deg/ °C)	0	-0.4	-0.3	-0.2	-0.4

Fig. 1. **T**he critical wetting temperature concept**: plot of** the right hand side of Eq.(1) **vs. temperature**, for various hydrophobized ceramic membranes characterized by different contact angles at 20 °C and by different **variations of θ with** temperature. No pore morphology variation with temperature. **Pure water.**

Remarkably, for each case, there is a temperature value at which the right hand side of Eq.(1) , $\gamma_{LV}\times|\cos\theta|$, **is** zero, which corresponds to the temperature at which the contact angle becomes 90 degrees: at that temperature the wetting process starts for each membrane pore, independently of the pore sizes, and, correspondingly, the LEP_{min} approaches the zero value. That temperature value represents the maximum operating temperature at which a hydrophobic membrane can operate in no-wetting conditions and it assumes the meaning of a critical temperature **for MD operations**

with a specific fluid: we propose to **denote** it as *the critical wetting temperature* ($T_{C\ wetting}$) of the membrane.

Apparently, in the case of pure water, the $T_{C\ wetting}$ is greatly **below** the critical temperature of **the substance** (374.15 °C) **at which the surface tension of the liquid approaches the zero value.** For all the cases studied, $T_{C\ wetting}$ can assume relatively low values**, with the exception of case A in which no variation of the contact angle with temperature is accounted.**

Although the concept of the critical wetting temperature has been put in evidence with reference to ceramic membranes, for which the hypothesis of no swelling is acceptable, it is important to observe that the same concept is valid also for polymeric membranes, in principle. In that case, however, the quantity plotted in Fig.1 might be expected to show a different behavior with temperature.

Eq.(1) can be used also to simulate the trend of LEP_{min} with temperature as a function of the maximum pore diameter. For the case D of Figure 1, for cylindrical pores (B=1), the simulations are reported in Figure 2: from another point of view, the existence of the critical wetting temperature can be observed and its independence of the pore size is reconfirmed.

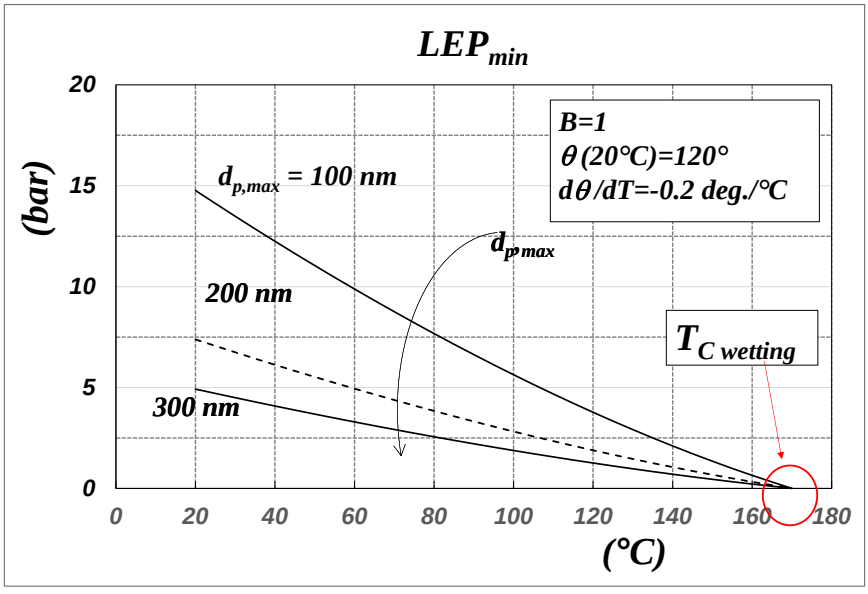

Fig.2. Simulation of LEP_{min} **with pure water** along temperature, according to Eq.(1), **at various maximum pore sizes. Cy**lindrical **pores, no pore morphology variation** with temperature (*B*=1).

Finally, by comparing the results of Figures 1 and 2, it can be observed that it is certainly advantageous to prepare low pore size membranes endowed with a high contact angle and with a

high LEP_{min} value **at room temperature**; however it is as much important to evaluate and/or **to** measure how the **temperature affects those properties.** Indeed, accounting for instance the cases B and D of Figure 1, it can be observed that the same critical wetting temperature **might be** obtained with membranes of different material**,** showing different contact angles at room temperature.

The concepts reported in Figures 1 and 2 require an experimental validation which can be adequately performed by measuring the dependence of LEP_{min} along the temperature in hydrophobized ceramic membranes, as it will be documented in the following sections.

3. MATERIALS AND METHODS

3.1 Membranes and modules

Carbon-based titania membranes were used, hydrophobized with FAS, manufactured by Fraunhofer Institute for Ceramic Technologies and Systems (IKTS, Hermsdorf, Germany) in cylindrical geometry, as tubular membranes and capillary membranes. Membranes are asymmetric, produced by a secondary growth of other layers on the lumen of a titania support. The basic ceramic membrane is a 4-layers membrane of decreasing pore sizes: the support is the outer layer (4500 nm pore size), followed by other 2 layers (30 μm thickness each, 800 nm and 250 nm pore size, respectively) and finally followed by the top layer (10 μm thickness and 100 nm nominal pore size) located at the lumen-side of the membrane. The manufacturing technique of the basic membrane was reported in [**42**] and most of the morphological characterization of each layer was documented in detail in [**43**], where SEM pictures were shown also.

The hydrophobic character is **obtained** by two techniques: the 4-layers membrane is firstly carbon-coated by the deposition and pyrolysis of a polymeric precursor and secondly surface-grafted with fluoroalchylsilane (FAS). Carbon-coating procedure was widely described by the manufacturer in the patent [**44**] and also documented in [**45,46**], whereas the grafting procedure with FAS (tridecafluoro-1,1,2,2 tetra-hydro-octyl-trichloro-oxysilane) was patented in [**47**].

Tubular samples were manufactured in the shape of "single channels", to allow testing the performances of a single membrane. A photographic documentation of the contact angle inside a single channel at room temperature is reported in the *Supplemental material*, in which the hydrophobic character of the inner surface of the membrane is confirmed by a value of 140.9

degrees, aligned with the values claimed by the manufacturer in [**44,47**]. Capillaries were produced according to the indications reported in [**48**] and arranged in un-baffled bundles.

Each cylindrical membrane, both single channels and capillaries, was refined by epoxy resin end-caps to prevent leakages of liquid across the annulus at the inlet section, from the lumen side towards the outer side. The same kind of epoxy resin was used by the manufacturer to seal each capillary on the ceramic plates of the bundle and to make the ceramic plates impermeable. All the relevant manufacturing details have been previously reported in [27], with regards to the single channels, and in [**49**], with regards to capillary bundles also. The morphological characterization of the same samples used in this work has been widely documented and discussed in [**49**] in which the mean pore diameter and the effective surface porosity **were** estimated by air permeation experiments. All the information relevant to the purposes of this work is summarized in Table 1.

Table 1. Morphological parameters and geometrical characteristics of samples

	morphological parameters				***geometrical characteristics***		
	support thickness (μm) (§)	*total thickness (μm) (§)*	*mean pore size (nm)(*)*	*effective surface porosity (m^{-1})(*)*	*Inner Diameter/ Outer Diameter of a membrane(§) (mm)*	*Number of tubular/capillary membranes*	*inner area (cm^2)*
single channels							
S2515	*1500*	*1570*	*259*	*1236*	*7/10*	*1*	*49.2*
S2516							
capillary bundles							
B2814	*580*	*650*	*n.a.*	*n.a.*	*1.90/3.20*	*37*	*442*
B2758			*87*	*5252*		*22*	*263*
B2888	*750*	*820*	*337*	*463*	*1.90/3.54*	*37*	*442*
B2940(#)		*835*	*368*	*424*	*1.87/3.54*		*435*

(§) from the manufacturer; (#)=45 μm thickness third layer (*) by gas permeation tests [**49**] ; (n.a.)= not available

It is important to point out that all the samples are made by the same basic material; the mean pore sizes indicate that all the samples are in the typical range of the **membranes** for MD purposes.

Single channels **(samples S2515 and S2516)** represent two different samples of the same membrane (same geometry and same mean pore size). Capillary bundles, on the contrary, represent samples of membranes of the same material with different geometrical characteristics (different inner diameter and thickness) and with different pore morphology (different mean pore sizes and effective surface porosity). Bundles containing 22 or 37 fibers were selected, in order to obtain overall mean performances of devices **which are** very similar to the final configuration of a membrane contactor.

3.2 Breakthrough conditions with pure water: protocols of measurements

The breakthrough conditions are measured according to the **systematic** method introduced and widely discussed by Varela-Corredor and Bandini in [27], where the equipment flow sheet and the protocols of measurements were explained in detail for the measurement**s** of the minimum Liquid Entry Pressure (LEP_{min}) and of the minimum Liquid Entry Temperature (LET_{min}).

For clarity sake, the main aspects of the methods are reported in the following, in order to support the comprehension of the experimental data and the discussion of the results.

Basic idea of LEP_{min} and LET_{min} measurements is that a membrane can be flooded with **a liquid solution** either by increasing the pressure difference across the membrane at constant temperature or by increasing the temperature at a constant value of the pressure difference **across the membrane**, respectively.

In order to evaluate the LEP_{min} **with water** in a wide range of temperatures, the volumetric flow rate (Q_p) of liquid demineralized water across the membrane is measured by increasing the transmembrane pressure (ΔP) **at constant temperature**. At temperatures lower than 70 °C, the liquid downstream the membrane is kept at atmospheric pressure along the whole measurement and the upstream pressure is progressively increased. At temperatures **from** 70 °C **to 140 °C**, on the contrary, the **measurement is to be performed at pressure values higher than the water vapor pressure at the corresponding temperature, to avoid evaporation. In those cases, the** pressure is initially regulated at a high value in both sides of the membrane **and subsequently** the ΔP across the membrane is **progressively** increased by decreasing the downstream pressure.

Data are collected to plot the "flooding curve" (Q_p vs. ΔP) and then elaborated to calculate the so-called "normalized volume flux", as represented in Eq. (2), **which has been introduced in** [27].

$$"normalized\ volume\ flux" \equiv \left.\frac{J_v\,\eta_w}{\Delta P}\right|_{at\ T} = \frac{Q_p(T)\,\eta_w(T)}{A_{IN}\,\Delta P} \qquad (2)$$

J_v represents the volume flux, calculated with reference to the inner surface area A_{IN} at the temperature T of the liquid, and η_w is the pure water viscosity at the same temperature.

As **discussed in [27], the "normalized flux" is a sort of membrane permeability accounting of the morphological parameters of the membrane, and, more precisely, it corresponds to the reciprocal of the membrane resistance of a microfiltration membrane; the definition of**

this quantity was introduced to compare results obtained at different temperatures in order to make the calculations uniform. As demonstrated in [27], at a constant temperature, the normalized flux is a function of ΔP and the shape of that function is typically formed by a rather constant horizontal curve followed by an increasing curve. The trends of the experimental data reported in Figures 3 and 4 document that behavior. The horizontal line accounts of the flow rate through the membrane "defects" (leakages across the end caps of the membrane, defects on the top-layer, etc.), according to a viscous motion across them; the increasing curve, on the contrary, accounts of the volumetric flow of the liquid across the flooded pores. The lower is the value of the normalized flux **at** the horizontal line, the better is the membrane for MD operations.

According to the normalized flux behavior, The LEP_{min} of a hydrophobic membrane was recognized as "*the lowest differential pressure value at which the normalized volume flux increases at constant temperature"* [27]. The value of LEP_{min} can be thus calculated following the graphical procedure represented by the relationships (3) and reported in Figure 3b), as an example.

$$LEP_{min} = P_A \pm \beta; \quad \sigma = \left|P_B - P_A\right| \Rightarrow P_A - \sigma \le LEP_{min} \le P_A \tag{3}$$

P_A is calculated as intersection between the straight line connecting the first two points of the increasing part of the flooding curve and the horizontal line; σ is the uncertainty of the measurement, related to the value of the pressure step set during the measurement; P_B **is** the last datum available before the increase of the flooding curve**;** β **is t**he instrumentation precision **(in this work** β=0.1 bar**)**.

In order to evaluate the LET_{min}, the volumetric flow rate (Q_p) of the liquid demineralized water is measured by increasing the liquid temperature and by keeping the transmembrane pressure (ΔP) as a constant value. Measurements are performed by keeping the liquid downstream the membrane at a pressure value higher than the water vapor pressure at the temperature under investigation **and by regulating the pressure upstream the membrane to keep the desired** ΔP **value**, following the protocols developed in [27]. In this case, the normalized volume flux can be plotted as a function of temperature, obtaining a behavior quite similar to the LEP_{min} case. As for the LEP_{min}, LET_{min} can be defined as "*the lowest temperature value at which the normalized volume flux increases at constant pressure difference across the membrane"[27]* and it can be calculated following the same kind of graphical procedure, represented by the relationships (4) and reported in Figure 5.

$$LET_{min} = T_A \pm \beta; \quad \sigma = \left|T_B - T_A\right| \Rightarrow T_A - \sigma \leq LET_{min} \leq T_A \tag{4}$$

In this work, the LET_{min} measurement was carried out by using a thermometer with a precision of (β=0.1 °C) and a differential manometer with a precision of 10 mbar.

Obviously, the two parameters are strictly related to each other: the value of LEP_{min} measured at a temperature T corresponds to the same breakthrough condition measured as $LET_{min} = T$ at a $\Delta P = LEP_{min}$. Both of them can be used, together or in alternative, to characterize a hydrophobic membrane and to define the applicability of it for **a** MD **process**.

Measurements of LEP_{min} or of LET_{min} were performed in this work, in the temperature range from 20 °C to 136 °C. Demineralized water (3-14 μS/cm at room temperature) was used in all the experiments. Different trials were performed with the same sample; trials are numbered in chronological order; after **each** flooding curve, the sample underwent a drying procedure in oven to regenerate the membrane for the **next** breakthrough experiment ([27]).

4. RESULTS AND DISCUSSION

This section documents the existence of a "critical wetting temperature", basing on the measurements of LEP_{min} and of LET_{min}, according to the procedures explained in the previous sections. Firstly, the flooding curves **are reported by plotting the normalized volume fluxes along the pressure or temperature and** the results of the calculations of LEP_{min} and of LET_{min} are documented. Finally, the experimental results are elaborated in order to put in evidence and to validate the concept of the critical wetting temperature **with pure water, for the membranes studied**.

LEP_{min} results

Normalized volume fluxes obtained with single channel samples and with bundles are reported in Figures 3 and 4, respectively. Figure 3b) **is a** detail of Figure 3a), aiming to show the explanation of the graphical calculation of LEP_{min} according to relationships (3). **All the r**esults of the LEP_{min} calculations are resumed in Table **2a**, for comparison.

With regards to single channels **(Figure 3)**, it is possible to observe that there is a good reproducibility of data**: t**he curves at the same temperature are rather **superimposed** in a wide

range of pressures**. In addition,** the horizontal lines give quite similar values, generally contained in very low ranges**; t**hose values **denote** a low extent of the defects both on the membrane surface

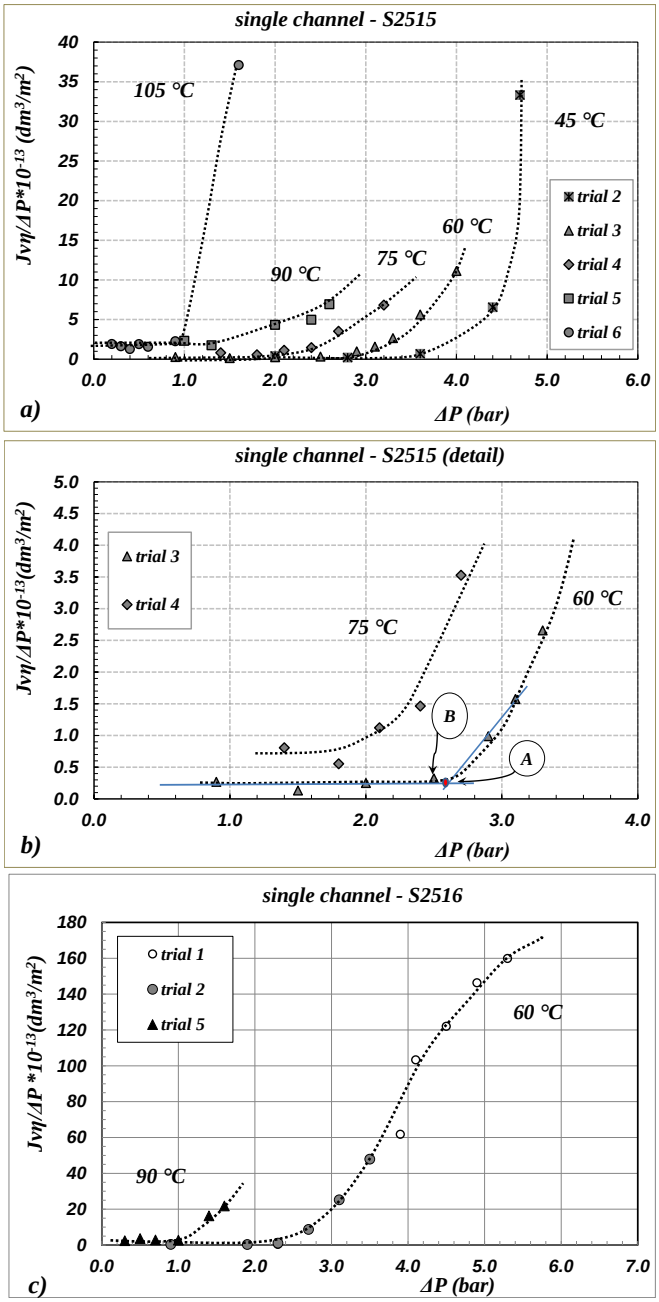

Fig.3. Single channel samples: "normalized volume fluxes" along the differential pressure across the membrane at constant temperature. (at 45 °C and 60°C pressure downstream the membrane = 1bar; at 75, 90 and 105°C pressure upstream the membrane=6.9 bar). (b) detail of Figure (a) showing also the graphical calculation of LEP_{min} (Eq.(3)).

and on the end-caps of the membrane and **therefore they document** a general good quality of the membrane **itsfelf**; they are also aligned with **the values** measured in [27] for other production **batches** of similar membranes.

Data reported in Figure 3 confirm that these two samples are representative samples of the same kind of membrane, as it had been put in evidence also by the gas permeation tests which **gave similar** mean pore size**s** and **similar** effective surface porosity values (see Table 1).

Also referring to the LEP_{min} values (as reported in Table **2a**), we can **confirm an interesting** reproducibility of **the** values **obtained**: **with regards** to the results at 60°C and 90 °C, **the** LEP_{min} values of samples S2515 and S2516 are different **by** 13 **and** 20%, respectively. In addition, by considering the whole set of results, these membranes show remarkably interesting LEP_{min} values in the range from 45 °C to 75 °C (3.5 bar and 2.0 bar, respectively), whereas a noticeable **drop in the** LEP_{min} is observed up to values **of 0.9** bar at 105 °C. The latter result, unfortunately, puts clearly in evidence that the applicability of those membranes **for MD processes** at temperatures higher than 105 °C is rather compromised**: in that case**, the **membranes can** operate in no-wetting conditions only **by keeping a total** pressure difference across t**hem below 0.9 bar**.

The flooding curves of bundles**,** reported in Figure 4, are equally interesting.

For bundles B2814 and B2940 (Figure 4a) the flooding curves are practically overlapped: although they were manufactured with small differences in the total thickness, **basing on that behavior** it is **possible to argue** that the fibers have a rather similar pore morphology, above all with regards to the maximum pore sizes. Conversely, the flooding curve of bundle B2758 **confirms** that in this **device** the fibers **morphology** is rather different **with respect to all the other samples**: **bundle B2758 shows** a very high LEP_{min} value of 6.9 bar at room temperature, which positively **matches** with a lower mean pore size, as obtained by gas permeation tests (Table 1).

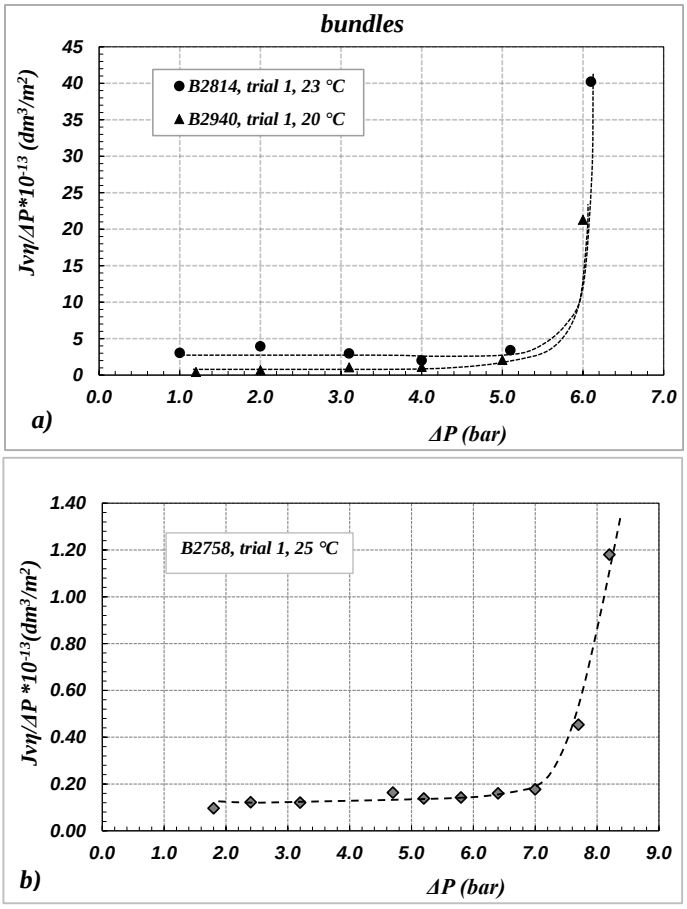

Fig.4. Capillary bundles: "normalized volume fluxes" along the differential pressure across the membrane at constant temperature (pressure downstream the membrane = 1 bar).

LET_{min} results

The flooding curve used to calculate the LET_{min} of bundle B2888 is reported in Figure 5; results are resumed in Table **2b** also. Experiments were carried out in the range from 95 to 136.6 °C; the corresponding operating pressures are reported in the table **in the right hand side of the** figure. The pressure difference across the membrane was regulated in the range from 0.30 to 0.40 bar along the measurement, with the exception of the data point at the highest temperature that was obtained at 0.03 bar. The **whole** experiment **required** three days.

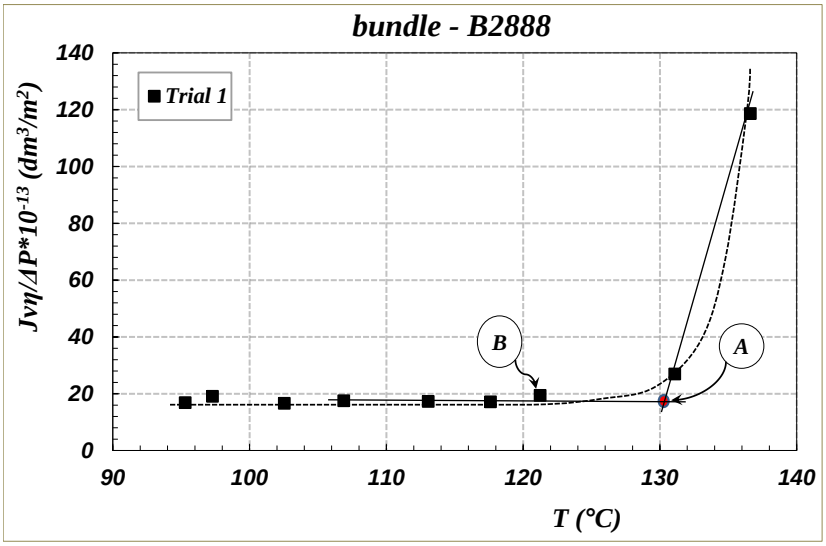

T (°C)	P_3 (bar)	ΔP (bar)
95.3	1.76	0.24
97.3	1.76	0.34
102.5	1.58	0.37
106.9	1.59	0.42
113.1	2.06	0.44
117.6	2.07	0.43
121.3	2.20	0.39
131.1	3.11	0.30
136.6	3.37	0.03

Fig. 5. *LET* measurement in a capillary bundle. "Normalized volume fluxes" vs. temperature. The corresponding pressure differences across the membrane are reported in the table. (P_3=pressure downstream the membrane). The graphical calculation of LET_{min} according to Eq.(4) is also reported.

Apparently, the normalized flux was recorded as a constant value up to 121 °C, in correspondence with a pressure difference of 0.39 bar across the membrane, and no wetting was observed (horizontal line). Subsequently, when the temperature was increased to 131°C and the pressure decreased to 0.30 bar, a slight increase of the normalized flux was detected, thus indicating that the breakthrough of the membrane was slightly in progress. **Evidence of w**etting **was observed as the** temperature was increased up to 136.6°C, at which a very high flux was measured in correspondence with 0.03 bar pressure difference.

That experiment allows to conclude that the LET_{min} of the bundle B2888 is contained in the range from 121.3 to 130.0 °C, when the pressure difference is kept in the range from 0.39 to 0.30 bar, respectively. Since at ΔP=0.03 bar the membrane is already on flooding conditions at 136 °C, we can easily extrapolate that a temperature in the range from 130 to 135 °C might correspond to the LET_{min} at zero pressure difference across the membrane. Therefore, reversing the meaning of LET_{min} into LEP_{min}, it is possible to conclude that the value of LEP_{min} close to zero can be estimated in the temperature range from 130 to 135 °C, which clearly corresponds to the maximum temperature at which the bundle can operate in no-wetting conditions **with pure water**.

Finally, by accounting of the theoretical premises discussed in the section 2, **it can be observed that** the LET_{min} at zero pressure difference across the membrane really corresponds to the "critical wetting temperature" of the membrane.

The critical wetting temperature

Data collected in Table 2 are plotted in Figures 6 according to different criterions.

Table 2. Characterization of hydrophobized carbon-based TiO_2 membranes according to the normalized flooding curve method (properties defined in Eqs (2)-(4))

Table 2a. ***LEP_{min} at constant temperature***

sample	***T***	σ	***LEP_{min}***	$Jv\big\vert_{at\ LEP_{min}}$	$Jv\eta/\Delta P\big\vert_{at\ LEP_{min}}$
	(°C)	***(bar)***	***(bar)***	***($dm^3/(hm^2)$)***	****10^{-13}(dm^3/m^2)***
	45.0	*0.6*	*3.5±0.1*	*0.03*	*0.20*
	60.0	*0.1*	*2.6±0.1*	*0.06*	*0.32*
S2515	*75.0*	*0.2*	*2.0±0.1*	*0.22*	*1.12*
	90.0	*0.2*	*1.2±0.1*	*0.25*	*1.74*
	105.0	*0.0*	*0.9±0.1*	*0.12*	*1.56*
S2516	*60.0*	*0.0*	*2.3±0.1*	*0.05*	*0.32*
	90.0	*0.0*	*1.0±0.1*	*0.32*	*2.80*
B2758	*25.0*	*0.5*	*6.9±0.1*	*0.04*	*0.16*
B2814	*23.0*	*0.1*	*5.2±0.1*	*0.72*	*3.40*
B2940	*20.0*	*0.0*	*5.0±0.1*	*0.16*	*1.11*

Table 2b. ***LET_{min} at constant pressure difference***

sample	***ΔP***	σ	***LET_{min}***	$Jv\big\vert_{at\ LET_{min}}$	$Jv\eta/\Delta P\big\vert_{at\ LET_{min}}$
	(bar)	***(°C)***	***(°C)***	***($dm^3/(hm^2)$)***	****10^{-13}(dm^3/m^2)***
B2888	*0.30-0.39*	*8.7*	*130.0±0.1*	*1.21*	*19.4*

In Figure 6a) the LEP_{min} values are reported along the temperature, accounting of the confidence range of the values represented by the vertical or by the horizontal bars, according to what has been described in relationships (3) and (4). The corresponding mean pore size values of each membrane/bundle are also reported (data from Table 1).

In Figure 6b) the same data are re-elaborated by plotting the corresponding values of the product $\frac{LEP_{\min} \times d_{P,mean}}{4}$ as a function of temperature, according to the premises of Eq.(1), by using the mean pore size values of Table 1.

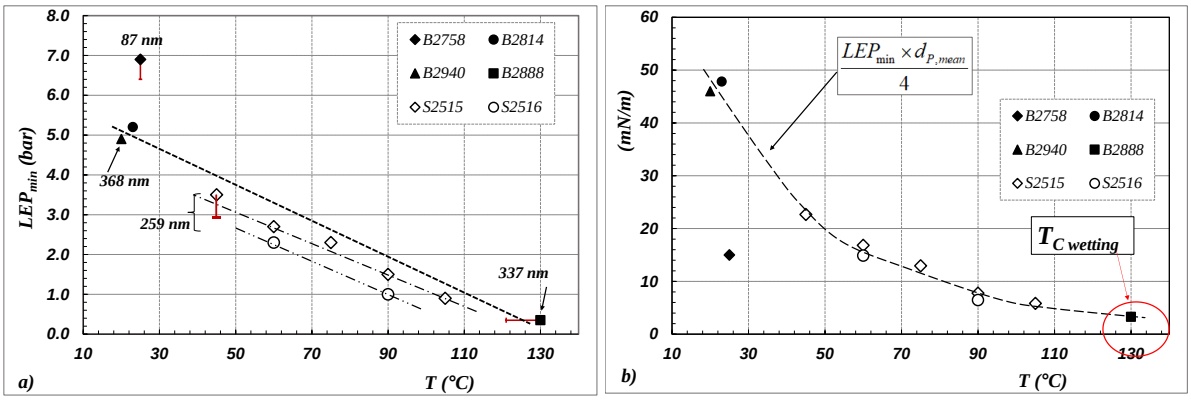

Fig. 6. **Experimental validation of the critical wetting temperature**. (a) Summary of LEP_{min} data vs. temperature for different samples (from Table 2), with the corresponding mean pore size values (from Table 1). (b) Elaboration of data reported in (a), according to the left side of Eq. (1).

All the samples were manufactured with the same ceramic material and hydrophobized according to the same procedure; they are different in the geometrical shape and are characterized by different morphologies (different membrane thicknesses, different mean pore sizes). The bundles showed LEP_{min} values intrinsically coherent with the **corresponding** pore size scale: the higher LEP_{min} **value is observed for** the lower mean pore size.

The data are therefore representative of the behavior of the breakthrough conditions with temperature of different hydrophobized ceramic membranes prepared with the same basic material; they clearly document the experimental evidence of the main aspects introduced and discussed in the theoretical **premises (**section 2):

1) The LEP_{min} is greatly affected by an increase of the liquid temperature (Figure 6a)**:** MD operations with this kind of membranes is rather compromised at temperatures higher than 110-130 °C, notwithstanding that the LEP_{min} values at room temperature are **greater** than 4 bar;
2) The existence of a maximum temperature at which the membrane can operate in no-wetting conditions is proved both in Figure 6a) and in Figure 6b). **T**he critical wetting temperature ($T_{Cwetting}$) of this kind of membranes is close to 130 °C **with pure water** and, remarkably,

it is independent of the pore size and only dependent on the membrane material (Figure 6b), as it **was** supposed according to Eq. (1) and represented in Figure 1. Since most of the data in Figure 6b) are aligned in the same curve, we can get an intrinsic confirmation of the agreement between experimentation and theoretical interpretation, **by the comparison between Figure 6b) and Figure 1, respectively. F**rom another **point of view,** we can **consider those data as** an important validation of the concept of the critical wetting temperature.

In addition, it is possible to conclude also that all the samples tested **had been** really manufactured with the same pore morphology (that is with the same value of the parameter *B* of Eq.(1)), with the exception of bundle B2758; **indeed,** on the contrary, data points of Figure 6b) would have been much more scattered.

Finally, it is interesting to put in evidence that the concept of $T_{Cwetting}$ seems to be complementary to the concept of "wetting surface tension" introduced in [50] to test the effect of alcohol-water solutions on membrane wetting. Authors [50] documented a "unique wetting surface tension for each type of membrane, independent of the type of alcohol", in a temperature range from 25 to 40 °C. The premises for the definition of the wetting surface tension relied on the assumption that the dispersion component of liquid surface tension and of the solid surface tension were independent of composition and of temperature. However Petke and Ray [35] documented a linear decreasing behavior of those quantities with temperature in a range from 20 to 120 °C, for various materials. Basing on those values, the wetting surface tension can be estimated as a decreasing function with temperature. As a consequence, only in the case in which temperature and composition affect the surface tension of the liquid and the contact angle in such a way to give the same LEP_{min} values, a unique value of wetting surface tension might be obtained corresponding to the wetting concentration and/or to the wetting temperature.

As a final comment, it is interesting to put in evidence that the data **range** reported in Figure 6b) is rather comparable with the theoretical simulations reported in Figure 1**, being** intermediate between the curves representing cases C and E**: t**he role of the contact angle and the importance of investigating its dependence with temperature is remarkably evident.

5. CONCLUSIONS

The most important innovation of this paper is the introduction and the discussion of the concept of the *critical wetting temperature* ($T_{Cwetting}$) of a hydrophobic membrane.

The concept relies on theoretical premises **of** the Laplace-Young equation, supported also by a literature documentation **about** the temperature effect on the contact angle of water on various materials. The parameter represents the maximum temperature at which a hydrophobic membrane can operate in no-wetting conditions **in the presence of an aqueous solution**, and it corresponds to the temperature at which the contact angle approaches the value of 90 degrees; correspondingly, the Liquid Entry Pressure (LEP_{min}) approaches the zero value, and the wetting process starts for each membrane pore, independently of the pore size. $T_{Cwetting}$ depends on the membrane material only and it is remarkably independent of the membrane pore size.

The knowledge of the critical wetting temperature is crucial to evaluate which operative conditions are more convenient for a membrane distillation process and, above all, which are the applicability limits of a membrane contactor as a hydrophobic device. It is a parameter which should be included in the membrane characterization protocols, since the **measurements** of the contact angle and of the Liquid Entry Pressure at room temperature cannot be sufficient to represent the real potentialities and the real limitations of the membrane.

The existence of the critical wetting temperature has been experimentally documented for the case of carbon-based titania membranes hydrophobized with FAS, by measuring the LEP_{min} values as a function of temperature, in the range from 20 °C to 130 °C. In that case, the $T_{Cwetting}$ was close to 130 °C **with pure water**; however, the applicability of those membranes **in MD processes** at temperatures higher than 105 °C **seems to be** rather compromised, since the membranes show LEP_{min} values **well below 1** bar at that temperature.

At present, the evaluation of $T_{Cwetting}$ can be performed as extrapolation **of** LEP_{min} data along temperature, which requires to **carry out** various experimental tests **for t**he same sample, **according to various flooding curves followed by cycles of drying procedures.** However, a rather good evaluation of that parameter can be obtained by performing the minimum *Liquid Entry Temperature* (LET_{min}) measurement at a very low pressure difference across the membrane (300 mbar, for instance), which can be carried out along one trial only. In the case in which it **is** possible to perform LET_{min} measurements at a pressure difference across the membrane very close to zero,

the $T_{CWetting}$ of that membrane might be obtained straightforwardly, **since it corresponds to the maximum value of LET_{min}. However, it is important to stress the difference between $T_{CWetting}$ and LET_{min} : the former is a property of the membrane material only with a specific solution, independent of the pore size, the latter is a property of the membrane which measures the breakthrough conditions as a function of the pressure difference across the membrane which generally depend on the pore size, as long as the pressure difference is greater than zero.**

Further verifications of these conclusions are certainly desired for other different kinds of membranes to confirm **and support the validity** of **the critical wetting temperature concept and to investigate how it is affected by the type of solution.**

AUTHORS CONTRIBUTIONS: ***Felipe Varela-Corredor***: conceptualization, methodology, experimental investigation, data elaboration and validation. ***Serena Bandini***: conceptualization, methodology, validation, funding acquisition and resources, writing-review and editing.

FUNDINGS: This research was partially supported by Saipem-S.p.A (Milan, Italy) in the framework of grants n. 658283 (2012-2015) and n.1040403 (2015-2017) with DICAM-University of Bologna and supported by the University of Bologna (ECOIBANDI2)

ACKNOWLEGMENTS

Authors gratefully thank Dr. Hannes Richter and Dr. Marcus Weyd (Fraunhofer Institute for Ceramic Technologies and Systems - IKTS, Hermsdorf, Germany), for their kind cooperation in the discussion of the results, and Drs. Michele Biccari and Riccardo Zauli for their cooperation in performing some experiments.

REFERENCES

[1] C. Picard, A. Larbot, E. Tronel-Peyroz, R. Berjoan, Characterisation of hydrophilic ceramic membranes modified by fluoroalkylsilanes into hydrophobic membranes, Solid State Sci. 6 (2004) 605–612.

[2] S.R. Krajewski, W. Kujawski, F. Dijoux, C. Picard, A. Larbot, Grafting of ZrO2 powder and ZrO2 membrane by fluoroalkylsilanes, Colloids Surfaces A Physicochem. Eng. Asp. 243 (2004) 43–47.

[3] S.R. Krajewski, W.M. Kujawski, M. Bukowska, C. Picard, A. Larbot, Application of fluoroalkylsilanes (FAS) grafted ceramic membranes in membrane distillation process of NaCl solutions, J. Memb. Sci. 281 (2006) 253–259.

[4] J.Lu, Y.Yu, J.Zhou, L.Song, X.Hu, A. Larbot, FAS grafted superhydrophobic ceramic membrane, Applied Surface Science 255 (2009) 9092-9099

[5] J. Kujawa, W. Kujawski, S. Koter, K. Jarzynka, A. Rozicka, K. Bajda, S. Cerneaux, M. Persin, A. Larbot, Membrane distillation properties of TiO2 ceramic membranes modified by perfluoroalkylsilanes, Desalin. Water Treat. 51 (2013) 1352–1361.

[6] S.Cerneaux, I.Struzynska, W.M.Kujawski, M.Persin, A.Larbot, Comparison of various membrane distillation methods for desalination using hydrophobic ceramic membranes, J. Membrane Science 337 (2000) 55-60

[7] S. Koonaphapdeelert, K. Li, Preparation and characterization of hydrophobic ceramic hollow fibre

membrane, J. Memb. Sci. 291 (2007) 70–76.
[8] S. Koonaphapdeelert, Z. Wu, K. Li, Carbon dioxide stripping in ceramic hollow fibre membrane contactors, Chem. Eng. Sci. 64 (2009) 1–8.
[9] L. García-Fernández, B. Wang, M.C. García-Payo, K. Li, M. Khayet, Morphological design of alumina hollow fiber membranes for desalination by air gap membrane distillation, Desalination 420 (2017) 226–240.
[10] C.-C. Ko, A. Ali, E. Drioli, K.-L. Tung, C.-H. Chen, Y.-R. Chen, F. Macedonio, Performance of ceramic membrane in vacuum membrane distillation and in vacuum membrane crystallization, Desalination 440 (2018) 48-58.
[11] Y.-R. Chen, L.-H. Chen, C.-H. Chen, C.-C. Ko, A. Huang, C.-L. Li, C.-J.Chuang, K.-L. Tung, Hydrophobic alumina hollow fiber membranes for sucrose concentration by vacuum membrane distillation, J. Memb. Sci. 555 (2018) 250-257.
[12] Y. Fan, S. Chen, H. Zhao, Y. Liu, Distillation membrane constructed by TiO2 nanofiber followed by fluorination for excellent water desalination performance, Desalination 405 (2017) 51-58.
[13] M.-Y. Yang, J.-W. Wang, L. Li, B.-B. Dong, X. Xu, S. Agathopoulos, Fabrication of low thermal conductivity yttrium silicate ceramic flat membrane for membrane distillation, J. of the European Ceramic Society 39 (2019) 442–448.
[14] P. Jacob, S.Laboire, C. Cabassud, Visualizing and evaluation wetting in membrane distillation: New methodology and indicators based on Detection of Dissolved Tracer Intrusion (DDTI), Desalination 443 (2018) 307-322
[15] P. Jacob, B. Dejean, S.Laboire, C. Cabassud, An optical in-situ tool for visualizing and understanding wetting dynamics in membrane distillation, J. Membrane Sci. 595 (2020) 117587
[16] M.Rezaei, D.M. Warsinger, M.Duke, T. Matsuura, W.M. Samhaber, Wetting phenomenon in membrane distillation: mechanisms, reversal, and prevention, Water Research 139 (2018) 329-352
[17] M.Gryta, Long-term performance of membrane distillation process, J. Membrane Sci. 265 (2005) 153-159
[18] M.Gryta, Influence of polypropylene membrane surface porosity on the performance of membrane distillation process, J. Membrane Sci. 287 82007) 67-78.
[19] J.Ge, Y.Peng, Z. Li, P.Chen, S.Wang, Membrane fouling and wetting in a DCMD process for RO brine concentration, Desalination 344 (2014) 97-107
[20] F.Edwwie, M.M.Teoh, T.S.Chung, Effects of additives on dual-layer hydrophobic –hydrophilic PVDF hollow fibers membranes for membrane distillation and continuous performance, Chem. Eng. Sci. 68 (2012) 567-578.
[21] H.Julian, S.Meng, H.Li, Y.Ye, V.Chen, Effect of operation paramenters on the mass transfer and fouling in submerged vacuum membrane distillation crystallization (VMDC) for inland brine water treatment, J.Membrane Sci. 520 (2016) 679-692
[22] E.Guillen-Burrieza, A.Ruiz-Aguirre, G.Zaragoza, H.A.Arafat, Membrane fouling and cleaning in long term plant-scale membrane distillation operations, J. Membrane Sci. 468 (2014) 360-372.
[23] R.B. Saffarini, B. Mansoor, R. Thomas, H.A. Arafat, Effect of temperature-dependent microstructure evolution on pore wetting in PTFE membranes under membrane distillation conditions, J. Memb. Sci. 429 (2013) 282–294.
[24] E. Guillen-Burrieza, A. Servi, B.S. Lalia, H.A. Arafat, Membrane structure and surface morphology impact on the wetting of MD membranes, J. Memb. Sci. 483 (2015) 94–103
[25] E. Drioli, A. Criscuoli, E. Curcio, Membrane contactors: fundamentals, applications and potentialities, Elsevier, Amsterdam (2006)
[26] M. Khayet, T. Matsuura, Membrane Distillation-Principles and Applications, Elsevier, 2011.
[27] F. Varela-Corredor, S.Bandini, Advances in water breakthrough measurement at high temperature in macroporous hydrophobic ceramic/polymeric membranes, J. Memb. Sci. 565 (2018) 72-84
[28] K.Simons, K.Nijmeijer, M.Wessling, Gas-liquid membrane contactors for CO2 removal, J. Memb. Sci. 340 (2009) 214-220
[29] D. Singh, K. Sirkar, Desalination of brine and produced water by direct contact membrane

distillation at high temperatures and pressures, J. Memb. Sci. 389 (2012) 380–388.

[**30**] A.C.M. Franken, J.A.M. Nolten, M.H.V. Mulder, D. Bargeman, C.A. Smolders, Wetting criteria for the applicability of membrane distillation, J. Memb. Sci. 33 (1987) 315–328.

[**31**] Bruce E. Poling; John M. Prausnitz; John P. O'Connell. Properties of Gases and Liquids, Fifth Edition, McGraw-Hill Education, 2001

[**32**] Design Institute of Physical Property Data bank- DIPPR; http://www.aiche.org/dippr

[**33**] M.C. Phillips, A.C. Riddiford, Temperature Dependence of Contact Angles, Nature. 205 (1965) 1005–1006.

[**34**] A.W. Neumann, Contact angle and their temperature dependence: thermodynamic status, measurement. Interpretation and application., Adv. Colloid Interface Sci. 4 (1974) 105–191.

[**35**] F.D. Petke, B.R. Ray, Temperature dependence of contact angles of liquids on polymeric solids, J. Colloid Interface Sci. 31 (1969) 216–227.

[**36**] A.W. Adamson, Potential distortion model for contact angle and spreading. II. Temperature dependent effects, J. Colloid Interface Sci. 44 (1973) 273–281.

[**37**] M.E. Diaz, M.D. Savage, R.L. Cerro, The effect of temperature on contact angles and wetting transitions for n-alkanes on PTFE, Journal of Colloid and Interface Science 503 (2017) 159-167

[**38**] J.D. Bernardin, I. Mudawar, C.B. Walsh, E.I. Franses, Contact angle temperature dependence for water droplets on practical aluminum surfaces, Int. J. Heat Mass Transf. 40 (1997) 1017–1033.

[**39**] T. Hayashi, T. Hazuku, T. Takamasa, K. Takamori, Contact Angle of Water Droplets in a High-Temperature, High-Pressure Environment, in: Proceedings of ICONE12 (12th International Conference on Nuclear Engineering, April 25-29, 2004, Arlington, Virginia, USA), (2004) ICONE12-49418

[**40**] W. Kujawski, J. Kujawa, E. Wierzbowska, S. Cerneaux, M. Bryjak, J. Kujawski, Influence of hydrophobization conditions and ceramic membranes pore size on their properties in vacuum membrane distillation of water-organic solvent mixtures, J.Membrane Science 499 (2016) 442-451

[**41**] M.Courel, E. Tronel-Peyroz, G.M.Rios, M.Dornier, M.Reynes, The problem of membrane characterization for the process of osmotic distillation, Desalination 140 (2001) 15-25.

[**42**] H.Richter, I.Voigt, G.Fischer, P. Puhlfürß, Preparation of zeolite membranes on the inner surface of ceramic tubes and capillaries, Separation and Purification Technology. 32 (2003) 133-138

[**43**] M. Weyd, H. Richter, P. Puhlfürß, I. Voigt, C. Hamel, A. Seidel-Morgenstern, Transport of binary water-ethanol mixtures through a multilayer hydrophobic zeolite membrane, J. Membrane Sci. 307 (2008) 239-248.

[**44**] H.Richter, S.Kaemnitz, J.Gruetzner, D. Martin, I. Voigt, Carbon membrane, process for the manufacture of carbon membranes and use thereof, US Patent n. US2016/0175767 A1, Fraunhofer and MUW Screentec Filter (DE), Jun. 23, 2016

[**45**] S. Zeidler, P. Puhlfürß, U. Kätzel, I. Voigt, Preparation and characterization of new low MWCO ceramic nanofiltration membranes for organic solvents, J. Memb. Sci. 470 (2014) 421–430.

[**46**] A.Pashkova, R.Dittmeyer, N.Kaltenborn, H.Richter, Experimental study of porous tubular catalytic membranes for direct synthesys of hydrogen peroxide, Chemical Engineering Journal. 165 (2010) 924-933

[**47**] I. Voigt, G.Dudziak, T. Hoyer, A.Nickel, P.Puhlfuerss, Membrana ceramica de nanofiltracao para a utilizacao em solvents organicos e processo para a sua preparacao, PT Patent n. PT 1603663 E, Fraunhofer (DE), deposited on Feb. 25, 2004.

[**48**] I. Voigt, G. Fischer, P. Puhlfürß, M. Schleifenheimer, M. Stahn, TiO2-NF-membranes on capillary supports, Sep. Purif. Technol. 32 (2003) 87–91.

[**49**] M.K. Fawzy, F. Varela-Corredor, S. Bandini, On the morphological characterization procedures of multilayer Hydrophobic Ceramic Membranes for Membrane Distillation operations, Membranes, 9 (2019) 125-139

[50] M.C. García-Payo, M.A. Izquierdo-Gil, C. Fernández-Pineda, Wetting study of hydrophobic membranes via liquid entry pressure measurements with aqueous alcohol solutions, J. Colloid Interface Sci. 230 (2000) 420–431.

Supplemental material

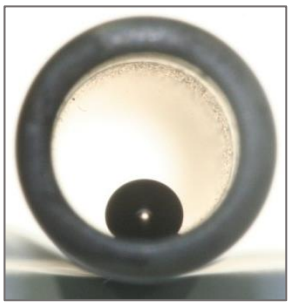

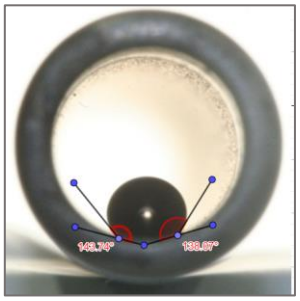

Contact angle of demineralized water at room temperature inside a single channel sample

Captions list of Figures

Fig. 1. **T**he critical wetting temperature concept**: plot of** the right hand side of Eq.(1) **vs. temperature**, for various hydrophobized ceramic membranes characterized by different contact angles at 20 °C and by different **variations of θ with** temperature. No pore morphology variation with temperature. **Pure water.**

Fig.2. Simulation of LEP_{min} **with pure water** along temperature, according to Eq.(1), **at various maximum pore sizes. Cy**lindrical **pores, no pore morphology variation** with temperature (B=1).

Fig.3. Single channel samples: "normalized volume fluxes" along the differential pressure across the membrane at constant temperature. (at 45 °C and 60°C pressure downstream the membrane = 1bar; at 75, 90 and 105°C pressure upstream the membrane=6.9 bar)
(b) Detail of Figure (a) showing also the graphical calculation of LEP_{min} (Eq.(3)).

Fig.4. Capillary bundles: "normalized volume fluxes" along the differential pressure across the membrane at constant temperature (pressure downstream the membrane = 1 bar).

Fig. 5. *LET* measurement in a capillary bundle. "Normalized volume fluxes" vs. temperature. The corresponding pressure differences across the membrane are reported in the table. (P_3=pressure downstream the membrane). The graphical calculation of LET_{min} according to Eq.(4) is also reported.

Fig. 6. **Experimental validation of the critical wetting temperature**. (a) Summary of LEP_{min} data vs. temperature for different samples (from Table 2), with the corresponding mean pore size values (from Table 1). (b) Elaboration of data reported in (a), according to the left side of Eq. (1).

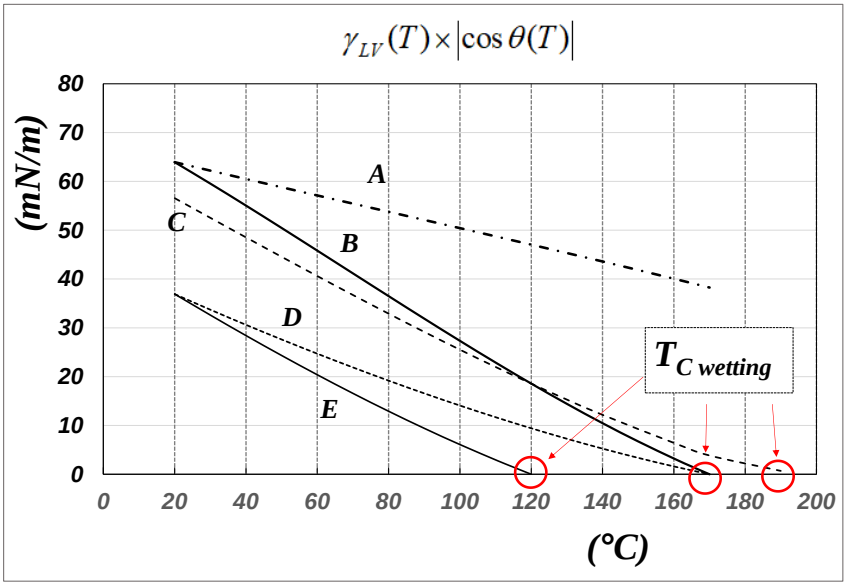

	A	B	C	D	E
θ @ 20°C (deg)	150 °	150 °	140 °	120 °	120 °
$d\theta/dT$ (deg/ °C)	0	-0.4	-0.3	-0.2	-0.4

Fig. 1. **T**he critical wetting temperature concept**: plot of** the right hand side of Eq.(1) **vs. temperature**, for various hydrophobized ceramic membranes characterized by different contact angles at 20 °C and by different **variations of θ with** temperature. No pore morphology variation with temperature. **Pure water.** .

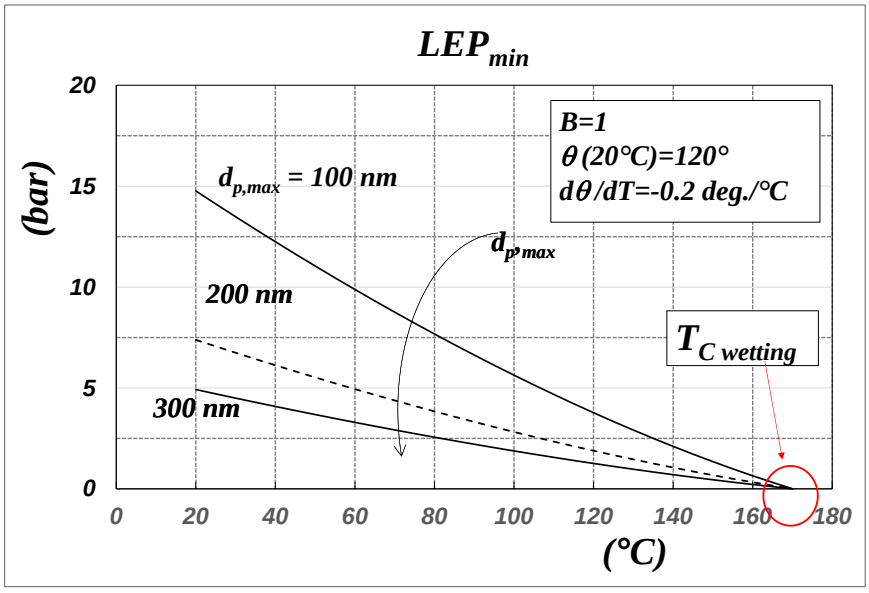

Fig.2. Simulation of LEP_{min} **with pure water** along temperature, according to Eq.(1), **at various maximum pore sizes. Cy**lindrical **pores, no pore morphology variation** with temperature (*B*=1).

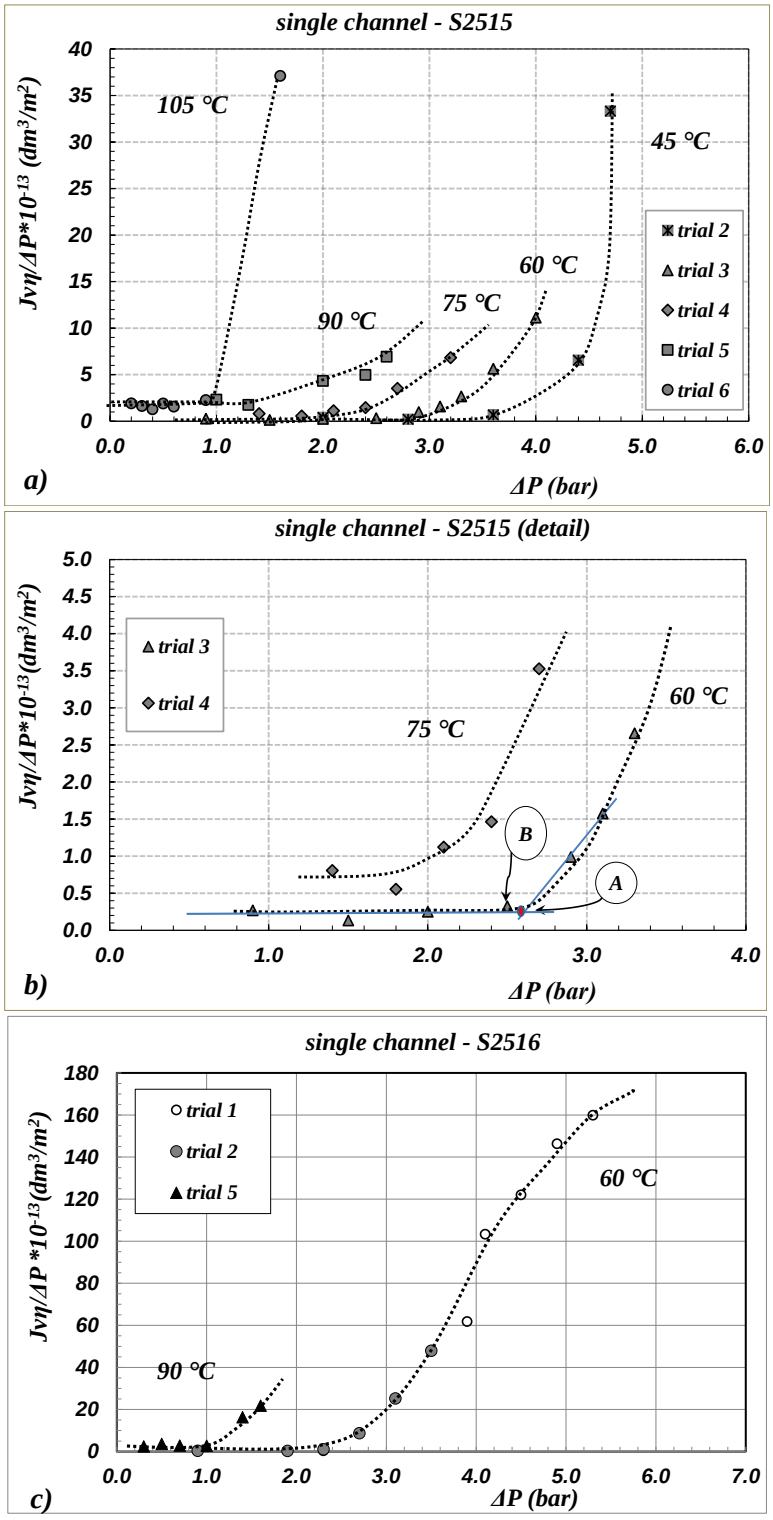

Fig.3. Single channel samples: "normalized volume fluxes" along the differential pressure across the membrane at constant temperature. (at 45 °C and 60°C pressure downstream the membrane = 1bar; at 75, 90 and 105°C pressure upstream the membrane=6.9 bar)
(b) detail of Figure (a) showing also the graphical calculation of LEP_{min} (Eq.(3)).

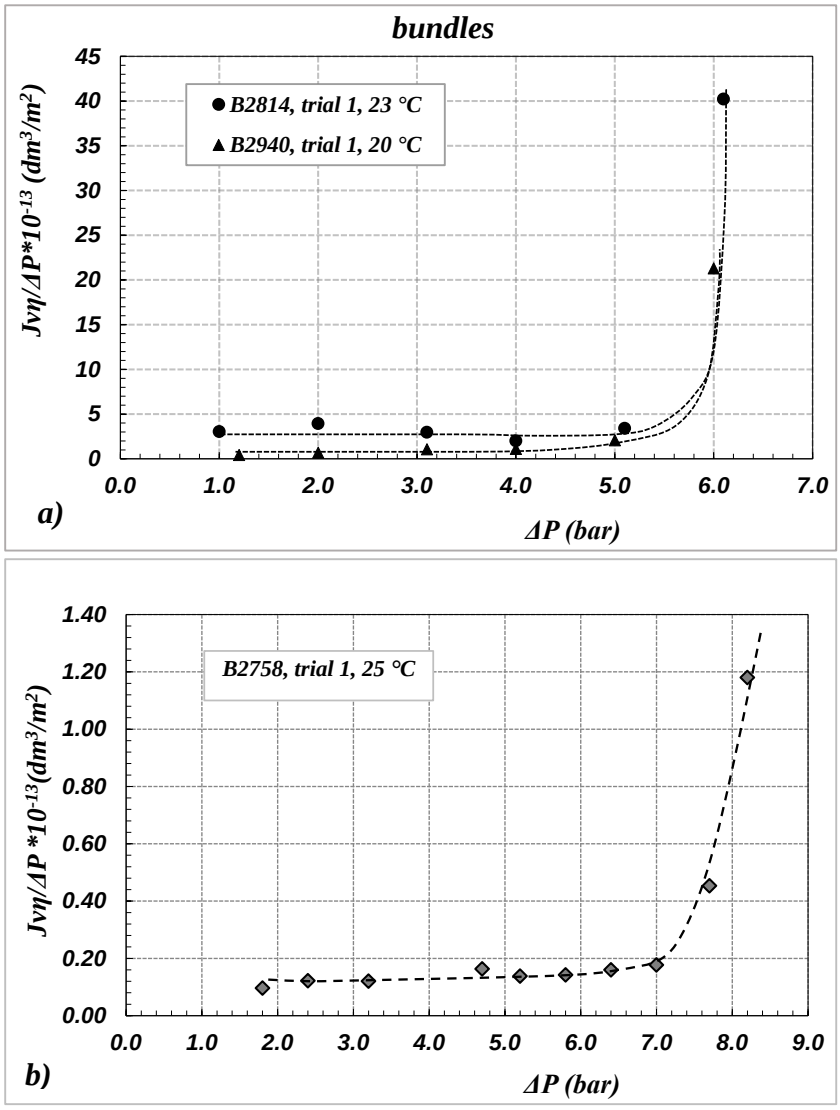

Fig.4. Capillary bundles: “normalized volume fluxes” along the differential pressure across the membrane at constant temperature (pressure downstream the membrane = 1 bar).

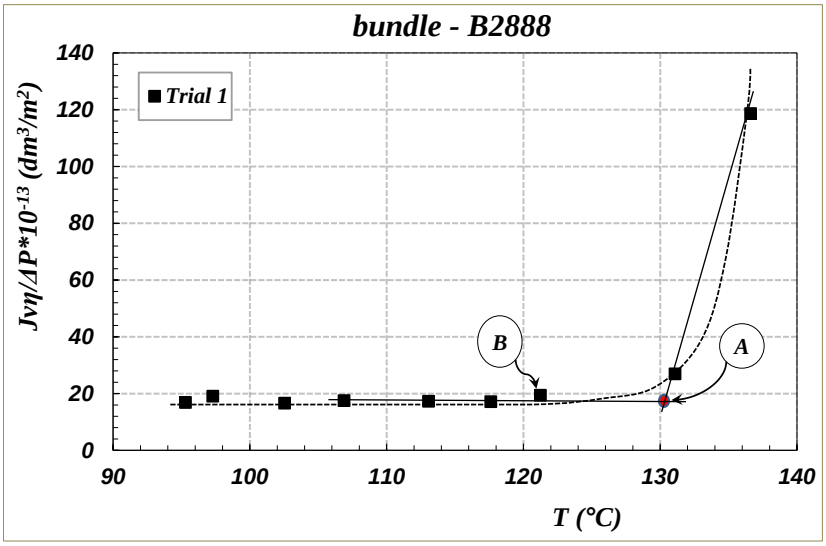

T (°C)	P_3 (bar)	ΔP (bar)
95.3	1.76	0.24
97.3	1.76	0.34
102.5	1.58	0.37
106.9	1.59	0.42
113.1	2.06	0.44
117.6	2.07	0.43
121.3	2.20	0.39
131.1	3.11	0.30
136.6	3.37	0.03

Fig. 5. *LET* measurement in a capillary bundle. "Normalized volume fluxes" vs. temperature. The corresponding pressure differences across the membrane are reported in the table. (P_3=pressure downstream the membrane). The graphical calculation of LET_{min} according to Eq.(4) is also reported.

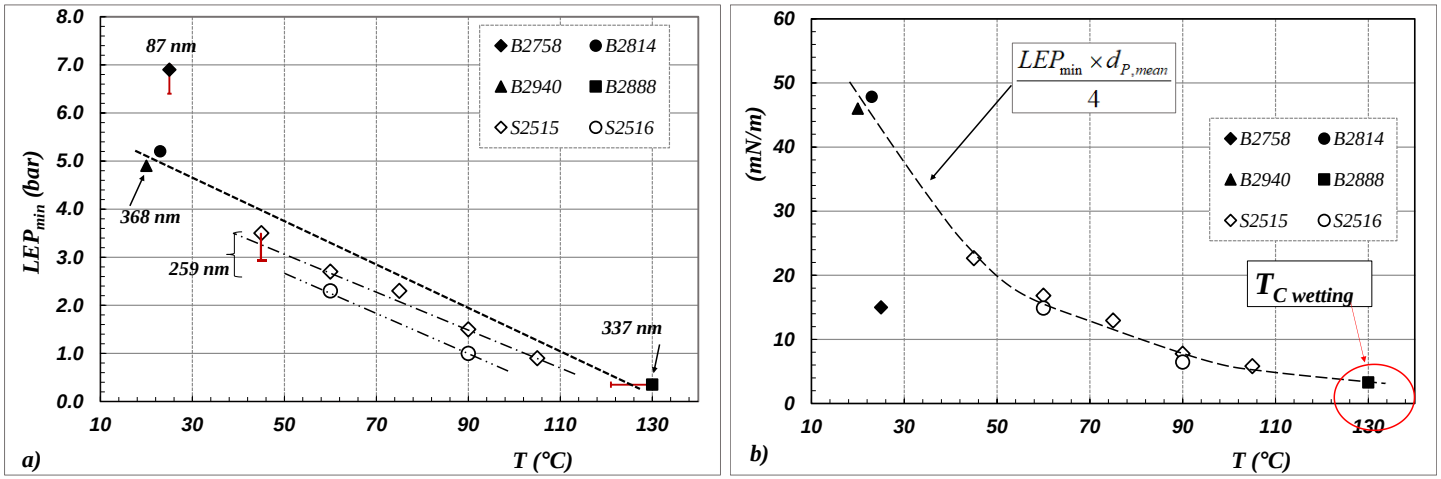

Fig. 6. **Experimental validation of the critical wetting temperature** (a) Summary of LEP_{min} data vs. temperature for different samples (from Table 2), with the corresponding mean pore size values (from Table 1). (b) Elaboration of data reported in (a), according to the left side of Eq. (1).

Tables

Declaration of interests

☒ The authors declare that they have no known competing financial interests or personal relationships that could have appeared to influence the work reported in this paper.

☐The authors declare the following financial interests/personal relationships which may be considered as potential competing interests:

AUTHORS CONTRIBUTIONS: ***Felipe Varela-Corredor***: conceptualization, methodology, experimental investigation, data elaboration and validation. ***Serena Bandini***: conceptualization, methodology, validation, funding acquisition and resources, writing, review and editing.